ORIGINAL ARTICLE

Distinct Corticostriatal and Intracortical Pathways Mediate Bilateral Sensory Responses in the Striatum

Ramon Reig and Gilad Silberberg

Department of Neuroscience, Karolinska Institute, Stockholm 17177, Sweden

Address correspondence to Gilad Silberberg, Department of Neuroscience, Karolinska Institute, Stockholm 17177, Sweden. E-mail: gilad.silberberg@ki.se

Abstract

Individual striatal neurons integrate somatosensory information from both sides of the body, however, the afferent pathways mediating these bilateral responses are unclear. Whereas ipsilateral corticostriatal projections are prevalent throughout the neocortex, contralateral projections provide sparse input from primary sensory cortices, in contrast to the dense innervation from motor and frontal regions. There is, therefore, an apparent discrepancy between the observed anatomical pathways and the recorded striatal responses. We used simultaneous in vivo whole-cell and extracellular recordings combined with focal cortical silencing, to dissect the afferent pathways underlying bilateral sensory integration in the mouse striatum. We show that unlike direct corticostriatal projections mediating responses to contralateral whisker deflection, responses to ipsilateral stimuli are mediated mainly by intracortical projections from the contralateral somatosensory cortex (S1). The dominant pathway is the callosal projection from contralateral to ipsilateral S1. Our results suggest a functional difference between the cortico-basal ganglia pathways underlying bilateral sensory and motor processes.

Key words: barrel cortex, corticostriatal pathways, in vivo whole-cell recordings, sensory integration, sensory striatum

Introduction

The striatum is the main input structure of the basal ganglia, receiving excitatory glutamatergic input from the neocortex as well as specific thalamic nuclei (Wilson 1987; Kincaid and Wilson 1996; Hoover et al. 2003; Alloway et al. 2009; Doig et al. 2010). Corticostriatal projections convey information from somatosensory (Donoghue and Herkenham 1986; Kincaid and Wilson 1996; Alloway et al. 1999; Pidoux et al. 2011; Wall et al. 2013; Reig and Silberberg 2014; Sippy et al. 2015), auditory (Znamenskiy and Zador 2013), and visual (Cui et al. 2013; Khibnik et al. 2014; Reig and Silberberg 2014) cortical regions. It was recently shown that projection neurons (MSNs) in the mouse dorsal striatum respond to tactile stimulation of both ipsi- and contralateral whiskers, with stronger and earlier responses mediated by stimulation of the contralateral whisker (Reig and Silberberg 2014). These differences between ipsi- and contralateral responses suggest that

they are mediated by different pathways, however, the detailed structure of these pathways is largely unknown.

Ipsilateral corticostriatal projections are prevalent throughout the neocortical sheet, including primary sensory, motor, and prefrontal cortical regions (Carman et al. 1965; Donoghue and Herkenham 1986). They are mediated by two main pathways, the pyramidal tract (PT) and the intratelencephalic tract (IT), which also projects to the contralateral striatum (Shepherd 2013). Conversely, contralateral corticostriatal projections of the IT pathways are sparser and more heterogeneous, with denser innervations in frontal cortical regions such as prefrontal and motor cortex, but very sparse or nonexistent in primary sensory areas (Carman et al. 1965; Donoghue and Herkenham 1986; McGeorge and Faull 1989; Brown et al. 1996; Alloway et al. 2006). These lateral differences in corticostriatal projections further suggest that ipsi- and contralateral sensory

responses in striatal neurons are mediated by different underlying pathways. In addition to the corticostriatal projections, striatal neurons receive excitatory inputs from thalamus (Smith and Bolam 1990; Doig et al. 2010; Wall et al. 2013; Alloway et al. 2014), however, it is not clear what is the role of the thalamostriatal projection in generating sensory responses, and in particular, the observed responses to brief whisker stimuli.

In this study, we used whole-cell striatal recordings combined with cortical extracellular recordings and selective blocking of primary somatosensory (S1) and motor (M1) cortical regions in order to elucidate the synaptic pathways underlying striatal integration of bilateral tactile sensory stimuli. Our data suggest that striatal responses to both ipsi- and contralateral whisker stimulation arise primarily from ipsilateral corticostriatal projections from S1. Interhemispheric propagation of the response is mediated primarily by callosal connections between S1 of both hemispheres rather than direct contralateral projections from S1 to dorsal striatum.

Materials and Methods

Ethical Approval

All experiments were performed according to the guidelines of the Stockholm Municipal Committee for animal experiments.

Electrophysiological Recordings

Both sex adult C57BL6 mice between 2 and 6 months were used to perform the experiments ($N = 40$). Anesthesia was induced by intraperitoneal injection of ketamine (75 mg/kg) and medetomidine (1 mg/kg) diluted in 0.9% NaCl. A maintaining dose of ketamine (30 mg/kg I.M.) was administrated every 2 h or after changes in the EEG or reflex responds to paw pinching. Animals were sacrificed after recordings by receiving an overdose of sodium pentobarbital (200 mg/kg I.P.). Tracheotomy was performed to increase the mechanical stability during recordings by decreasing breathing-related movements. Mice were placed in a stereotaxic device and air enriched with oxygen was delivered through a thin tube placed 1 cm from the tracheal cannula. Temperature was maintained between 36 and 37.5 °C using a feedback-controlled heating pad (FHC, Inc.). Craniotomies were made at three sites for patch clamp and extracellular recordings: AP 0 mm from Bregma, L 3.75 mm (striatum); AP 2 mm, L 2 mm (M1); AP −1.5 mm, L 3.25 mm (S1).

Whole-cell patch clamp recordings were obtained from dorsolateral striatum, between 2022 and 2375 μm deep from the pia, in a 30° angle. Signals were amplified using MultiClamp 700B amplifier (Molecular Devices) and digitized at 20 KHz with a Cambridge Electronic Design (CED) acquisition board and Spike 2 software (Cambridge Electronic Design). Patch pipettes were pulled with a Flaming/Brown micropipette puller P-87 (Sutter Instruments) and had an initial resistance of 5–12 MΩ, with longer tips than the standard ones to minimize cortical damage. Pipettes were backfilled with intracellular solution containing the following (in mM): 105 K-gluconate, 30 KCl, 10 Na-Phosphocreatine, 10 HEPES, 4 ATP-Mg, 0.3 GTP-Na, and 0.4% neurobiotin.

Extracellular recordings were obtained using tungsten electrodes with impedances of 1–2 MΩ. The electrodes were placed in infragranular layers in M1 and S1 with an angle between 15° and 25°. Recordings were amplified using a Differential AC Amplifier Model 1700 (A-M Systems) and digitized at 10 KHz with CED and Spike 2 simultaneously with the whole-cell recording.

Stimulation Protocols

Whisker stimulation was obtained by brief air puffs delivered by a picospritzer unit (Picospritzer III, Parker Hannifin) via 1 mm diameter plastic tubes placed at ~20 mm in front of the whiskers of both sides. Air puffs (15 ms duration) were given at least 40 times for each stimulus condition (ipsilateral, contralateral, or bilateral stimulation) with low frequency (0.2 Hz). Air pressure was equal for air puffs in both sides, and was set to 20 p.s.i. The whisker displacement following air puff was monitored and was determined to occur 11.0 ± 0.1 ms following the trigger command. The reference onset time for whisker deflection was therefore determined as 11 ms following the air puff trigger command. The presentation order for the three stimulus conditions (ipsi-, contra-, and bilateral whisker deflection) was randomized.

Analysis

"Up" and "Down" states were extracted from membrane potential recordings using an algorithm described by (Seamari et al. 2007). Sensory responses were classified according to those occurring during Up or Down states, including cases in which sensory stimulation triggered state transitions (Reig and Sanchez-Vives 2007). Stimuli were given at regular intervals (0.2 Hz) and therefore the probability that they occurred at different periods of the cycle reflected the time spent by the network in Up and Down states. As described previously, responses during Down states were larger and more reliably detected due to the stable baseline preceding the response and the increased driving force (Reig and Silberberg 2014). We therefore describe only data obtained from Down states. The onset of the evoked sensory responses was calculated as the average time between the stimulus trigger and the onset of the evoked potential of at least 40 stimuli presented at 0.2 Hz. We used the first and second time derivative of the membrane potential to determine the onset and peak of the sensory response within a 150 ms time-window after whisker stimulation. Response amplitude was defined as the voltage difference between the peak and onset potentials and slopes were obtained as dv/dt between the onset and peak time interval. Unless mentioned explicitly, all statistical tests performed were Student's t-test following the Shapiro-Wilk normality test for all compared data points. Error bars presented in the graphs represent the standard error of the mean.

Anatomy

Anterograde Tracing

Tracer injections were made using glass pipettes (borosilicate, OD = 1.5 mm, ID = 1.18 mm) with a tip diameter of 5–10 μm. Around 150–250 nl of BDA 10% (10 000 MW lysine-fixable biotin dextran amine, Molecular Probes) dissolved in 0.9% NaCl and fast green (to aid visualization of the injected tracer). Injections were performed in layer 5 of M1 and S1 using the coordinates described above. A single injection was done for each cortical area and animal using the coordinates described above. Following injection, we sealed the skin with surgical veterinary glue (3 M Vetbond Veterinary Tissue Adhesive 1469SB). The analgesic carprofen (Rimadyl; Pfizer) was administered subcutaneously at 5 mg/kg, and mice were awakened with intraperitoneal injections of a mixture of atipamezole (Antisedan; Orion Pharma; 1 mg/kg) and naloxone (0.1 mg/kg) diluted in 0.9% NaCl. Mice were then returned to the animal facilities in separate cages. After 3–6 days animals were transcardially perfused with a solution containing 4% formalin and 14% saturated picric acid

dissolved in 0.1 M phosphate buffer (PB, pH 7.4). Brains were extracted and stored in this fixative solution during 24–48 h. Before cutting, brains were transferred into PBS containing 12% sucrose for 24 h. Coronal slices (20 μm thick) of both hemispheres containing the entire striatum (from AP 1.7 mm to AP −2.3 mm were obtained using a cryostat and collected on gelatin coated slides. Sections were incubated over night with Cy3-conjugated streptavidin (Jackson ImmunoResearch Laboratories) and NeuroTrace 500/525 Green Fluorescent Nissl Stain (Invitrogen) diluted (1:1000) in 1% BSA, 0.3% Triton-X 100 in 0.1 M PB for axonal and somatic stain, respectively. For pictures in Figures 1 and 2, Nissl Stain was represent in blue and Cy3 in red. Finally, the glass slides were covered with glycerol containing 2.5% diazabicyclo octane (Sigma).

TTX and Tracer Injections

To study the neural connectivity underlying the striatal sensory response for the ipsilateral whisker stimulation, we injected tetrodotoxin (TTX) 10 μM with 0.4% neurobiotin dissolved in ringer solution in order to assess the spread of the injected solution (Figs 3B, 5B, 6B). Injections were made in upper layer 5 of contralateral M1 (AP 1.2 mm, L 1.5 mm) and in contra- and ipsilateral S1 (AP −1.5 mm, L 3.25 mm). The lateral spread of neurobiotin in these injections ($n = 28$) was 1038 ± 262 μm and the depth below pia was 895 ± 103 μm. We recorded the tactile responses in the striatum for ipsi- and contralateral whisker stimulation before and after TTX application. Injections were done using glass pipettes. In order to visualize neurobiotin staining following TTX injections, 20–25 μm thick coronal slices from
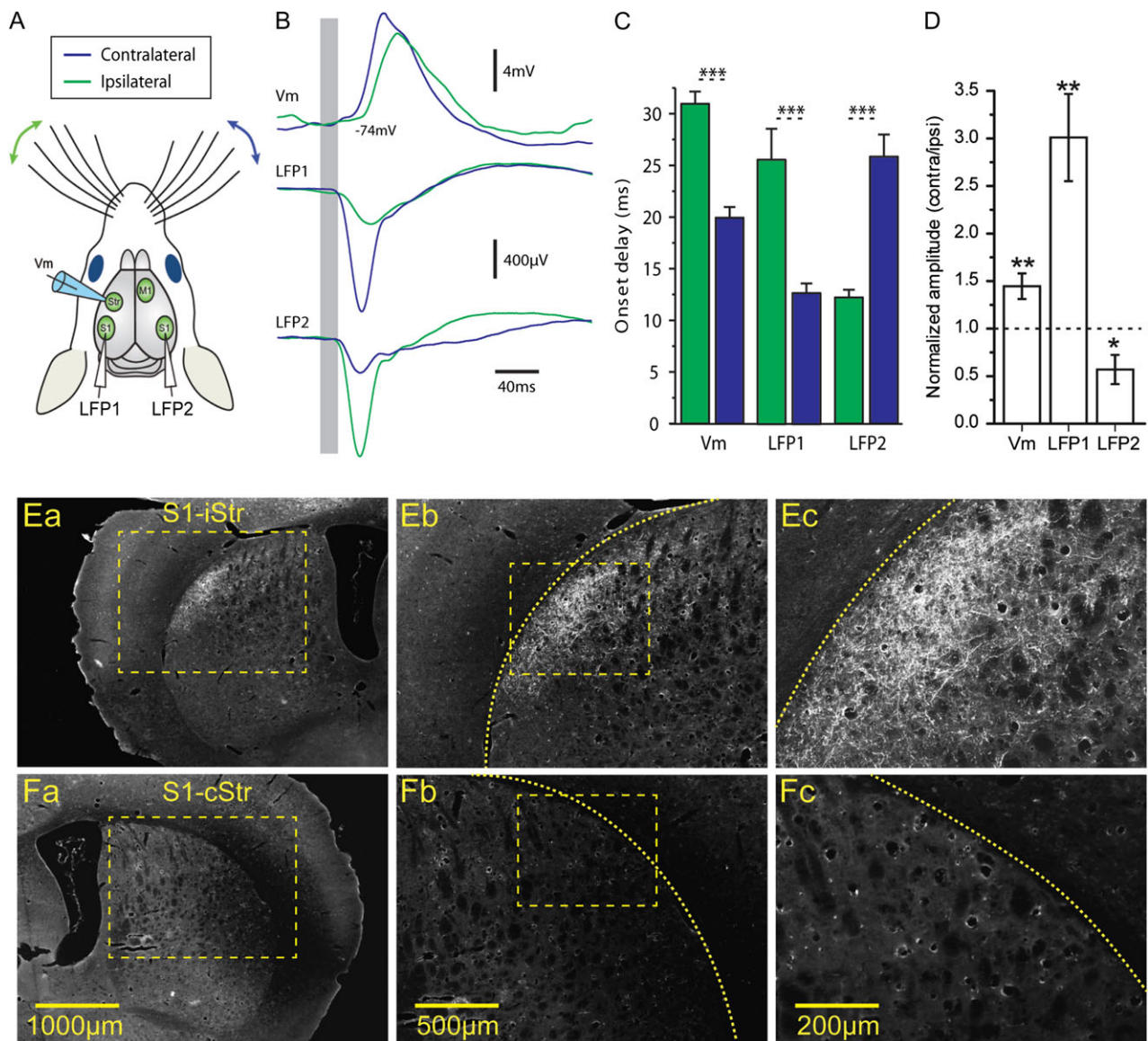
Figure 1. Bilateral whisker stimulations evoke responses in cortical S1 and dorsolateral striatum. (A) Scheme of the experimental setup. Whole-cell recordings were obtained from dorsolateral striatum simultaneously with extracellular LFPs recorded in the ipsi- and contralateral barrel fields in S1 (LFP1 and LFP2, respectively). (B) Responses to whisker deflection as recorded in the striatum (whole-cell recording, "top"), ipsilateral S1 (LFP1, "middle"), and contralateral S1 (LFP2, "bottom"). Presented traces are averages of 40 repetitions. (C) Onset delay, responses in both S1 and dorsolateral striatum were several milliseconds earlier for contralateral whisker stimulation. (D) Responses to contralateral whisker deflection were larger than those to ipsilateral stimulation, as measured in simultaneous whole-cell recordings in striatum and bilateral LFP recordings in S1. (E). Ipsilateral corticostriatal projections from S1 to dorsolateral striatum labeled by anterograde labeling (BDA-10000) in S1, shown at increasing magnifications (a–c). (F) Example of contralateral striatum receiving no corticostriatal projections from S1, as shown at increasing magnifications (a–c).
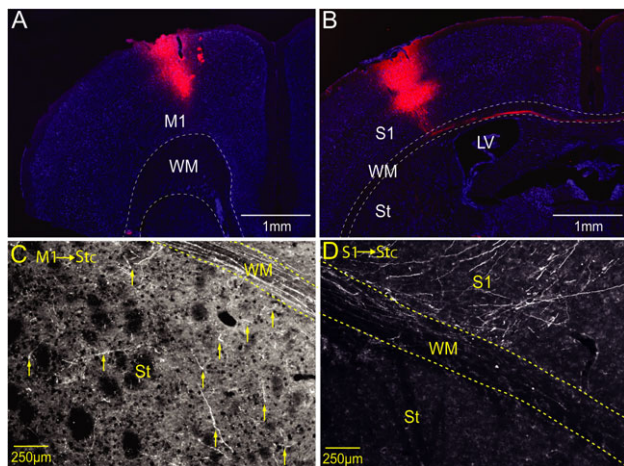
Figure 2. Contralateral corticostriatal projections are denser from M1 than S1. (*A*) Injection-site (BDA-10000 in red) in M1 at +1.2 mm a.p. from Bregma. (*B*) Injection-site in S1 (barrel field) at −1.5 mm a.p. from Bregma. Note the cortico-callosal projection to the contralateral hemisphere in the white matter. (*C*) Projection from M1 (shown in A) to the contralateral striatum. The yellow arrows show examples of axonal projections in dorsolateral striatum. (*D*) Projection from S1 (shown in B) to contralateral S1. Note the axons ascending from WM to cortex, and the lack of axonal projections in the striatum. BDA-10000 anterograde labeling for axonal projections presented in red, and Nissl stain for cell bodies in blue.

the injected hemisphere containing the cortical areas (M1 from AP 2.2 mm to AP −1 mm, and S1 from AP 0.3 mm to AP −2 mm) were obtained using a cryostat. The tissue was processed using the same protocol described for the BDA injections, but in this case we used Cy2-conjugated streptavidin (Jackson ImmunoResearch Laboratories). We only analyzed recordings in which we could visualize neurobiotin staining with a minimal spread of 500 μm surrounding the injected cortical area (For M1 n = 15 of 17 experiments; for contralateral S1 n = 7 of 8; and for ipsilateral S1 n = 6 of 7 different experiments). In these experiments, only one cell per animal was recorded before and after TTX injection.

Results

In order to study the role of corticostriatal projections in striatal sensory integration, we obtained whole-cell recordings from neurons in dorsal striatum and studied their responses to bilateral whisker stimulation. In addition to the whole-cell recordings, we obtained simultaneous extracellular field recordings from the barrel field in primary somatosensory cortex (S1) of both of both cortical hemispheres (Fig. 1*A*). Responses to brief air puffs to the whisker pads were observed at all recording sites, with clear differences between ipsi- and contralateral responses (Fig. 1*B–D*). Cortical local field potentials (LFPs) in S1 were earlier and stronger following stimulation of the contralateral whisker, than responses to ipsilateral stimulation (onset delay: LFP1 ipsi- = 25.6 ± 10.34 ms, LFP1 contra- = 12.69 ± 3.24 ms, LFP2 ipsi- = 12.21 ± 2.46 ms, LFP2 contra- = 25.81 ± 7.12 ms, $P < 0.001$ in both comparisons, see Figure 1*C*. Amplitude: LFP1 ipsi- = −206.2 ± 93.78 μV, LFP1 contra- = −624.58 ± 495.37 μV, LFP2 ipsi- = −620.97 ± 494.93 μV, LFP2 contra- = −256.73 ± 331.16 μV, $P < 0.01$ in both comparisons, Figure 1*D*, N = 13 animals). A similar relationship was observed in whole-cell striatal recordings, where contralateral responses were 11 ms earlier and 44% larger than responses to ipsilateral stimulation (Fig. 1*C,D*). We then used anterograde labeling in the cortex to study the cortical projection patterns in the dorsal

striatum (see "Materials and Methods" section). Corticostriatal projections from S1 were abundant and readily observed in the dorsolateral part of the ipsilateral striatum (Fig. 1*E*). Projections were also seen in the ipsilateral primary motor cortex (M1) and the contralateral S1. Contralateral corticostriatal projections from S1 were, however, extremely sparse and seen only in caudal striatum and most cases nonexistent at all (Figs. 1*F* and 2*D*, n = 5 animals). In contrast, projections from M1 were found throughout both striatal hemispheres (Fig. 2*C*, n = 5 animals). In summary, we found that S1 and M1 both project to the ipsilateral striatum but whereas M1 has a prominent contralateral projection, the contralateral corticostriatal projection from S1 is extremely sparse. This anatomical result together with the observed differences between ipsi- and contralateral response onset latencies (on average longer than 10 ms, Fig. 1*C*) suggests that responses to ipsilateral whisker deflection may be mediated by additional synapses, rather than by direct corticostriatal projections from contralateral S1.

We therefore wanted to establish whether contralateral S1 is necessary for mediating the striatal responses to ipsilateral whisker stimulation. To that end we injected 10 μM TTX in the barrel field of contralateral S1, thus blocking outputs from that cortical region (see "Materials and Methods" section and Fig. 3). In this set of experiments, we simultaneously obtained extracellular recordings from both ipsi- and contralateral S1 as well as whole-cell recordings from striatum during whisker stimulation (Fig. 3*A*). In the striatum, response amplitudes for ipsilateral stimulation were reduced in all recorded neurons following TTX injections in contralateral S1 (control 9.03 ± 2.26 mV; TTX 10 μM 1.98 ± 1.11 mV, $P < 0.001$, N = 7. Fig. 3*D,E*). In contrast, responses to contralateral whisker stimulation were not affected by TTX application (control 15.4 ± 7.88 mV, TTX 10 μM 14.05 ± 5.96, $P = 0.28$, Fig. 3*D,E*). As expected, the amplitudes of extracellular responses in contralateral S1 were reduced for both ipsi- and contralateral stimulation (LFP2 normalized amplitude for contralateral stimulation 0.24 ± 0.28, ipsilateral stimulation 0.06 ± 0.07, bilateral stimulation 0.12 ± 0.09, $P < 0.001$ in all cases, Fig. 3*F*). In ipsilateral S1 (Fig. 3*A*, LFP1), however, only responses evoked by ipsilateral whisker stimulation were decreased after TTX application (LFP1 normalized amplitude: contralateral stimulation 1.08 ± 0.21; ipsilateral stimulation 0.2 ± 0.16, $P < 0.001$; bilateral stimulation 1.0 ± 0.2). These results show that cortical and striatal responses to ipsilateral whisker stimulation are primarily mediated via the contralateral barrel cortex in S1. However, in face of previous studies and our own data above, the ipsilateral striatal responses are not likely to be mediated by direct corticostriatal projection but rather from additional parallel projections originating from contralateral S1.

The rodent primary somatosensory cortex excites the ipsilateral M1 (Hoffer et al. 2005; Ferezou et al. 2006; Matyas et al. 2010), which in turn, projects bilaterally to both striatal hemispheres. We wanted to test the possibility that the striatal response to ipsilateral whisker stimulation is mediated via contralateral M1 (Fig. 5). In order to confirm the functionality of projections from S1 to M1, we obtained simultaneous extracellular recordings (LFP) in M1 and S1 and recorded the evoked responses induced by whisker stimulation (Fig. 4). Responses were earlier in S1 compared with M1 for all stimulation protocols (Fig. 4*C–E*), thus confirming previous results (Matyas et al. 2010). Response amplitudes and slopes were also larger in S1 with respect to M1 (Fig. 4*F,G*). To directly assess the participation of M1 in mediating ipsilateral sensory responses, we
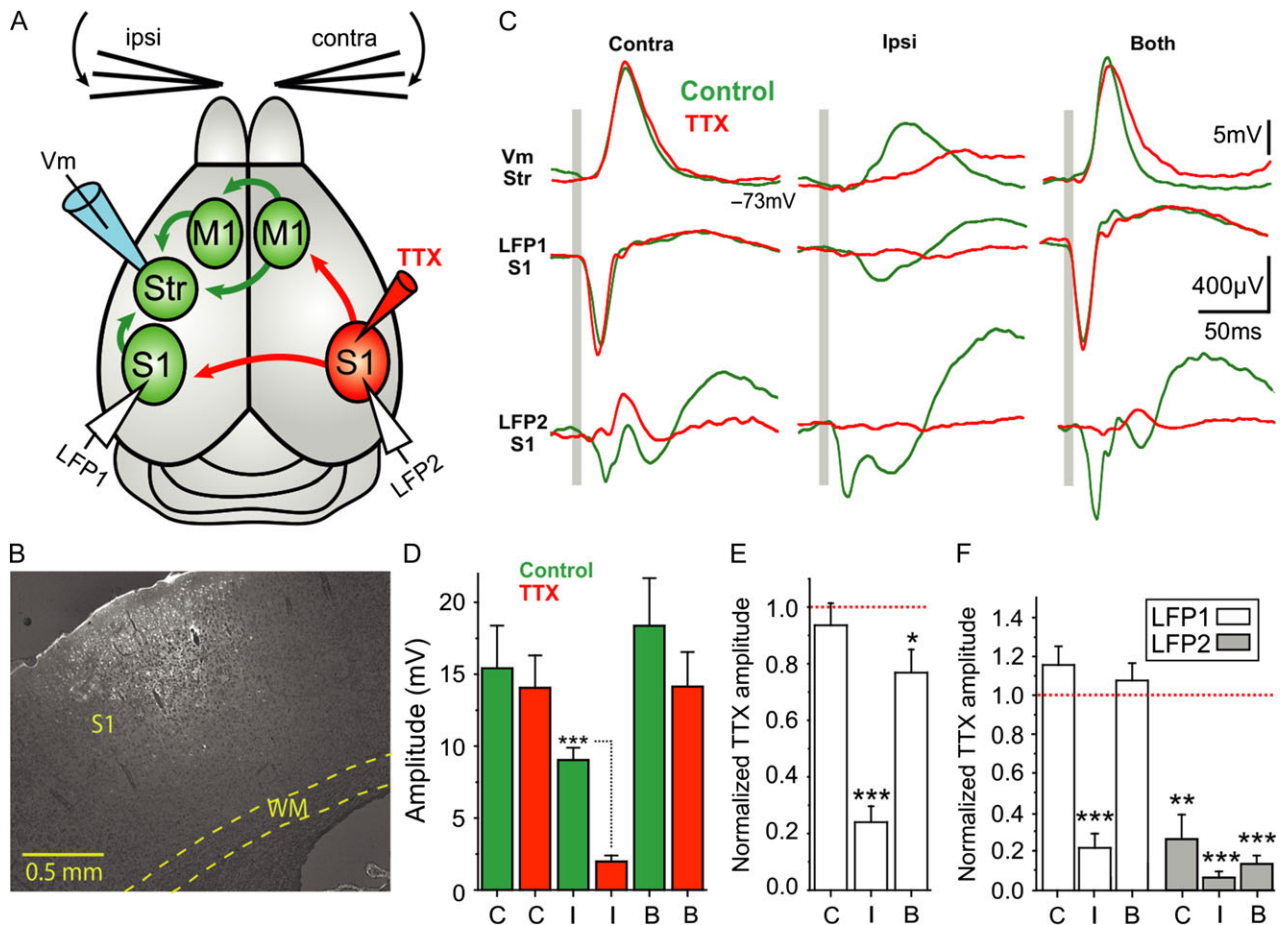
Figure 3. Contralateral S1 mediates striatal responses to ipsilateral whisker stimulation. (A) Diagram of the experimental configuration and main synaptic pathways; arrows in red show the synaptic outputs blocked by TTX injection to contralateral S1. Unblocked regions and pathways (green) and recording electrodes in dorsolateral striatum and S1 of both cortical hemispheres. (B) Example of a TTX (10 μM) and neurobiotin (0.4%) injection-site in contralateral S1. (C) Waveform average (>40 repetitions) of a whole-cell recorded MSN with simultaneous cortical LFP recordings in response to contra-, ipsi-, and bilateral whisker deflection before and after injection of TTX 10 μM in contralateral S1. The gray bar represents the air-puff whisker deflection. (D) Absolute response amplitude to contra-, ipsi-, and bilateral whisker deflection (n = 7 animals). (E) Normalized amplitude change in striatal whole-cell recordings. The normalization was done with respect to the control condition for each neuron and type of stimulation (n = 7). (F) Normalized amplitude with respect to the control condition for each LFP recording in the right and left cortical hemisphere and type of stimulation (n = 7). All responses are measured during down states. Asterisks *, **, *** represent P values <0.05, <0.01, <0.001, respectively.

recorded the responses to whisker stimulation before and after blocking the outputs from contralateral M1 with TTX 10 μM (Fig. 5). The immediate (up to 150 ms) response amplitude was not significantly reduced after TTX injections in contralateral M1 (ipsi-: control 9.78 ± 3.91 mV, TTX 10 μM 8.21 ± 3.38 mV; contra-: control 10.06 ± 5.86 mV, TTX 10 μM 8.98 ± 5.91 mV; N = 14, Fig. 5D,E). Application of TTX in contralateral M1 did, however, affect the late component of the ipsilateral whisker response, more than 150 ms following whisker deflection (9 cases out of 14, Fig. 5C). This decrease in the late component is likely caused by reducing cortical recurrent activity triggered by the sensory input, which in some cases also induced UP states (Anderson et al. 2000; Hasenstaub et al. 2007; Reig and Sanchez-Vives 2007; Alenda et al. 2010).

Another projection from S1 is a cortico-callosal projection to the contralateral S1 (Wise and Jones 1976; Akers and Killackey 1978; Hubener and Bolz 1988; Shuler et al. 2001; Innocenti et al. 2002; Le Be et al. 2007). We tested the possibility that a cortico-callosal S1–S1 pathway is involved in mediating the striatal response to ipsilateral whisker stimulation. Layer V neurons in S1 were previously shown to discharge action

potentials in response to stimulation of contralateral whiskers (de Kock et al. 2007; Pidoux et al. 2011), and we wanted to test whether similar stimulation would induce such suprathreshold responses in the opposite S1 as well. All three types of whisker deflection (contra-, ipsi-, and bilateral) evoked action potentials in layer 5 pyramidal neurons whole-cell recorded in S1 (see Supplementary Fig. S1). Response onset latencies were shorter following contralateral stimulation than those evoked by ipsilateral stimulation (34.98 vs. 71.87 ms, see Supplementary Fig. S1C), and the probability of evoking APs was higher for contralateral and bilateral stimulation than for ipsilateral stimulation (see Supplementary Fig. S1D). We then obtained striatal and cortical recordings before and after blocking ipsilateral S1 by application of TTX 10 μM (Fig. 6). Following TTX injection, striatal responses were largely attenuated in all neurons, for both contralateral and ipsilateral stimulations (reduction of 84 ± 17% and 61 ± 24%, respectively, P < 0.05, N = 6, Fig. 6D,E). Cortical extracellular field responses in S1 of the ipsilateral hemisphere, where TTX was applied (LFP1 Fig. 6A), were fully blocked for all stimulation protocols (ipsilateral: 99 ± 4%, contralateral: 96 ± 9%, bilateral: 92 ± 19%, Fig. 6F). However, field responses in
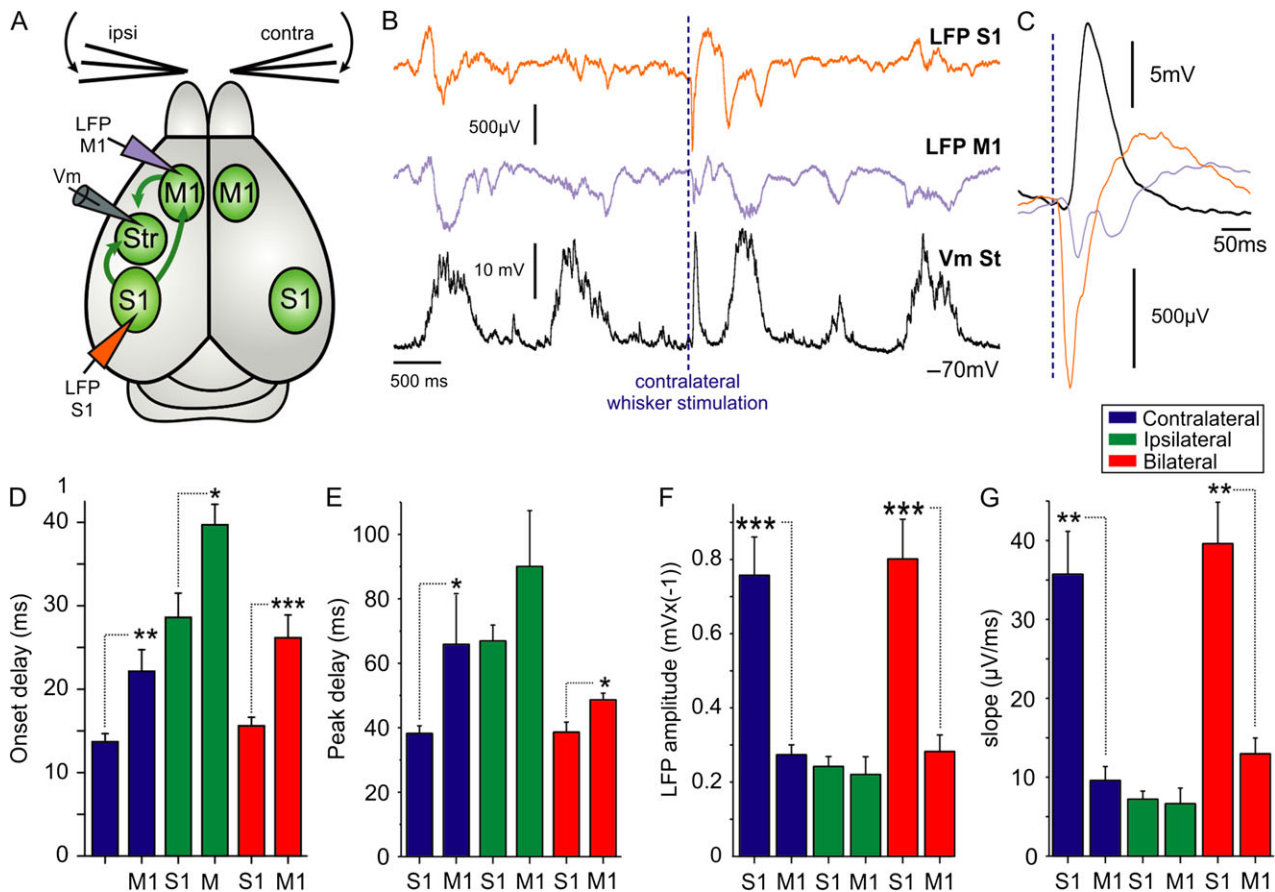
Figure 4. Whisker deflection activates M1 after the initial response in S1. (A) Diagram of the experimental configuration and synaptic projections; arrows illustrate the ipsilateral synaptic pathways mediating striatal responses to whisker deflection. Extracellular recording electrodes were placed in ipsilateral S1 and M1. (B) Simultaneous LFP recordings were obtained from S1 and M1, and a whole-cell voltage recording from a striatal MSN in the same hemisphere. The dashed line indicates the contralateral whisker stimulation. (C) Waveform average of responses to contralateral whisker deflection (>40 repetitions) for the recordings showed in B. Average responses in S1 and M1 for onset delay (D), peak delay (E), amplitude (F), and slope (G), N = 7. Asterisks *, **, *** represent P values <0.05, <0.01, <0.001, respectively.

contralateral S1 (LFP2 Fig. 6A) were blocked only for stimulation of the contralateral whisker (reduced by 99 ± 2%) and not for those evoked by ipsilateral stimulation (−1 ± 58%). These results mirror the one shown above, where activity in contralateral S1 was blocked by TTX (Fig. 3F). Bilateral whisker stimulation was partly blocked (41 ± 32%. Fig. 6F) reflecting the contribution of ipsilateral stimulation to the LFP2 responses. It is important to note that although responses to whisker stimulation were reduced, MSNs did receive other excitatory inputs, as seen in the ongoing spontaneous activity after TTX application in ipsilateral S1 (see Supplementary Fig. S2). Moreover, whisker responses were not fully blocked following TTX application in ipsilateral S1, suggesting the involvement of other parallel pathways underlying the residual responses. This final set of experiments also suggests that under our experimental conditions, thalamostriatal input has a minimal contribution to striatal responses, and does not act as an independent "shortcut" to the dominant cortical response.

In summary, our data show that individual striatal neurons respond to tactile sensory inputs from both whiskers, and that the main source for these responses is of cortical origin. Responses to contralateral whisker stimulation are mediated via direct ipsilateral projections from S1. In contrast, responses to ipsilateral stimulation are mediated by additional cortico-cortical connections within and between cortical hemispheres, originating from contralateral S1.

Discussion

In this study, we used in vivo whole-cell recordings combined with pharmacological inactivation in the cortex and anatomical tracing to study the corticostriatal pathways mediating the integration of bilateral tactile sensory information. Our data show that responses to ipsilateral whisker stimulation are mainly mediated by indirect projections from the contralateral S1. This is in contrast with responses to contralateral whisker stimulation, which are mediated by a direct corticostriatal input from the ipsilateral S1. We show that blocking ipsilateral S1 suppresses responses to contralateral whisker deflection, thus indicating that, under our experimental conditions, direct and independent thalamic input does not contribute to these sensory responses. Blocking ipsilateral S1 also suppressed most of the response to ipsilateral whisker stimulation, further showing that these responses are largely mediated by cortico-callosal projections between S1 of both cortical hemispheres. Our findings show that bilateral tactile responses in striatum are mediated by highly asymmetrical pathways, involving different types of synapses and cortical processing. Taking into account the dense contralateral corticostriatal arborization from frontal and motor regions, we propose that striatal participation in sensory integration is qualitatively different from motor-related corticostriatal processes.
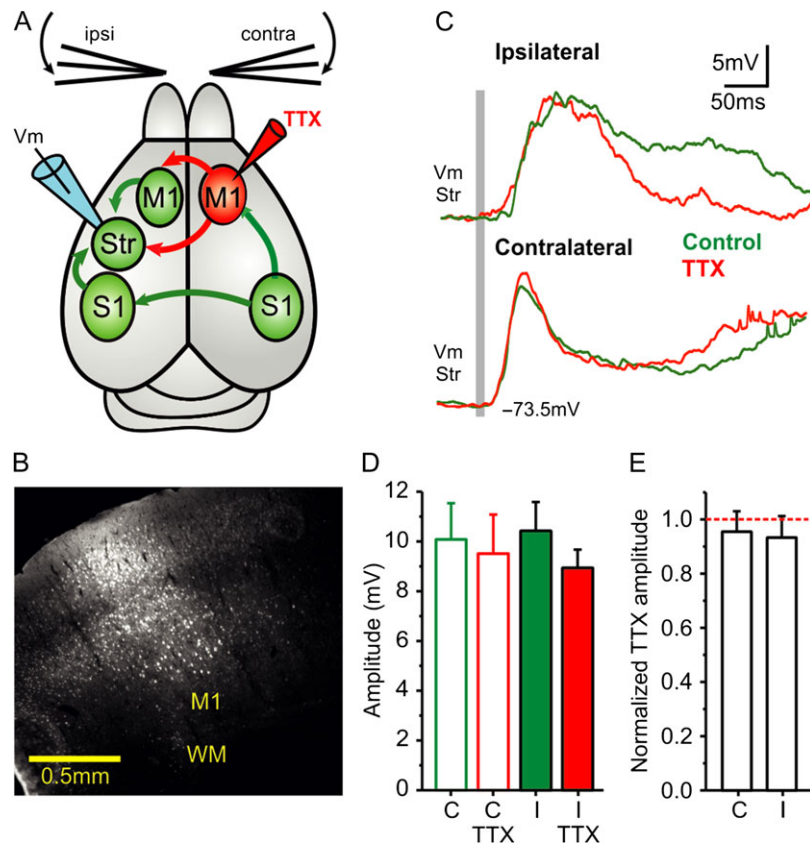
Figure 5. Blocking contralateral M1 does not affect striatal response to ipsilateral whisker stimulation. (A) Diagram of the experimental configuration and main synaptic pathways; arrows in red show the synaptic outputs blocked by TTX injection to contralateral M1. Unblocked regions and pathways are shown in green, the recording electrode in dorsolateral striatum in blue, and the TTX injection in M1 of the contralateral cortical hemisphere marked in red (see also Fig. S1). (B) Example of a TTX (10 μM) and neurobiotin (0.4%) injection-site in contralateral M1. (C) Waveform average (>40 repetitions) of a whole-cell recorded MSN in response to contra- and ipsilateral whisker deflection before and after injection of TTX in contralateral M1. The gray bar represents the air-puff whisker deflection. (D) Response amplitudes to contralateral and ipsilateral whisker deflection ($n = 14$). (E) Normalized response amplitudes. The normalization was done with respect to the control condition for each neuron and type of stimulation ($n = 14$). All responses are measured during down states. Asterisks *, **, *** represent P values <0.05, <0.01, <0.001, respectively.

Corticostriatal and Cortico-Cortical Pathways Mediate Striatal S1 Responses

Striatal neurons receive excitatory inputs from both cortical hemispheres, with ipsilateral projections being denser than contralateral ones and present for the entire cortical mantle (Carman et al. 1965; Kunzle 1975; Graybiel and Ragsdale 1979; McGeorge and Faull 1987; Wilson 1987). In contrast, contralateral projections are sparser and display a rostro-caudal gradient, with primary sensory cortices barely projecting to the contralateral striatum (Donoghue and Herkenham 1986; Brown et al. 1996; Alloway et al. 2006). Recent studies describing synaptic properties of the contralateral corticostriatal pathway (IT-type) were only performed in motor and frontal, but not primary sensory cortices (Morishima and Kawaguchi 2006; Kress et al. 2013). Direct contralateral projections from S1 to striatum do exist but are sparse and reported to originate from the septa between the cortical whisker barrels (Akers and Killackey 1978; Wright et al. 2001; Alloway 2008). Responses of striatal neurons to electrical stimulation in the contralateral S1 were reported to be slower and variable (Wright et al. 2001), which may also be explained by a disynaptic excitation via cortico-cortical synapses and not only by direct activation of the IT corticostriatal projection. Here, we showed that information from S1 indeed reaches striatum,

however, it is conveyed mainly by parallel cortico-cortical pathways and to a much lesser extent via direct contralateral corticostriatal projection from S1.

The barrel cortex projects to the contralateral cortical hemisphere via the cortico-callosal pathway (Wise and Jones 1976; Akers and Killackey 1978; Welker et al. 1988), which was shown to be essential in mediating cortical responses to whisker deflection (Shuler et al. 2001). In those experiments, whisker deflections could evoke spikes in S1 of both hemispheres, with responses to ipsilateral whisker deflection occurring with lower probability and longer latency (see Supplementary Fig. S1). Following unilateral inactivation of contralateral S1, all ipsilateral responses were abolished in the intact S1 (Shuler et al. 2001), further supporting our findings that S1–S1 callosal connections mediate the ipsilateral striatal response. In our experiments, inactivation of ipsilateral S1 blocked ~84% and ~61% of striatal responses to contralateral and ipsilateral responses, respectively, as recorded in the same neurons (Fig. 6E). This difference in the degree of blockage, as measured in the same neurons, may be attributed to the divergence in cortico-callosal and corticostriatal projections (Wise and Jones 1976), activating neighboring cortical regions beyond the TTX-affected region in S1. The residual response may also be mediated by the sparse contralateral corticostriatal axons originating from the barrel septa,
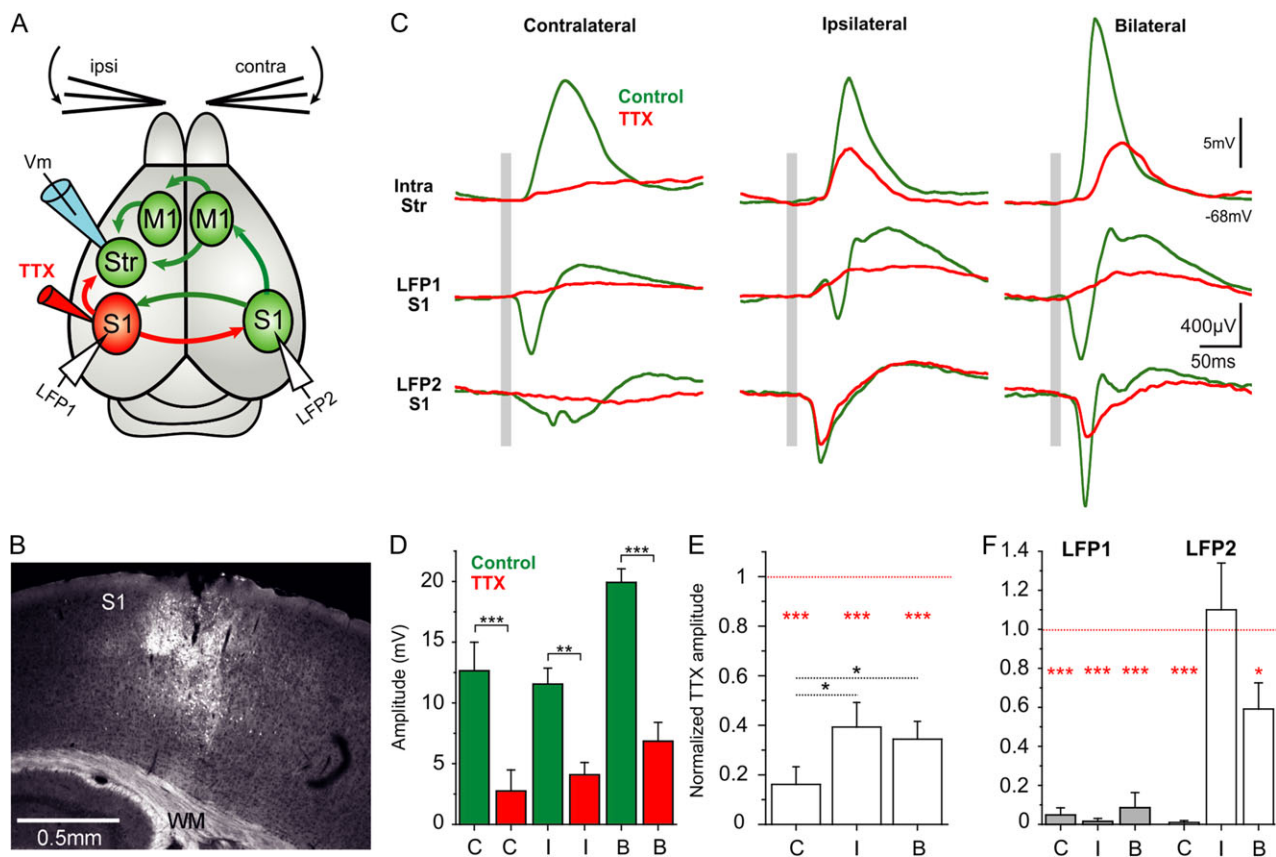
Figure 6. Blocking ipsilateral S1 reduces responses to both ipsi- and contralateral whisker stimulation. (A) Diagram of the experimental configuration and main synaptic pathways; arrows in red show the synaptic outputs blocked by TTX injection to ipsilateral S1. Unblocked regions and pathways (green) and recording electrodes in dorsolateral striatum and S1 of both cortical hemispheres. (B) Example of a TTX (10 μM) and neurobiotin (0.4%) injection-site in ipsilateral S1. (C) Waveform average (>40 repetitions) of a whole-cell recorded MSN with simultaneous cortical LFP recordings in response to contra-, ipsi-, and bilateral whisker deflection before and after injection of TTX 10 μM in ipsilateral S1. The gray bar represents the air-puff whisker deflection. (D) Absolute response amplitude to contra-, ipsi-, and bilateral whisker deflection before and after TTX application in ipsilateral S1 ($n = 6$ animals). (E) Normalized amplitude change in striatal whole-cell recordings. The normalization was done with respect to the control condition for each neuron and type of stimulation ($n = 6$). (F) Normalized amplitude with respect to the control condition for each LFP recording in the right and left cortical hemisphere and type of stimulation ($n = 6$). All responses are measured during down states. Asterisks *, **, *** represent P values <0.05, <0.01, <0.001, respectively.

which project to both ipsi- and contralateral striatal hemispheres (Wright et al. 2001).

Inactivation of contralateral M1 showed that it did not significantly contribute to the striatal responses to either ipsi- or contralateral whisker deflections (Fig. 5). Whisker deflection evokes delayed responses in contralateral M1, with significantly reduced amplitudes and slopes (Fig. 4), which may explain the minimal contribution of M1 to the contralateral striatal response. Inactivation of the contralateral M1 did, however, reduce later components of the ipsilateral whisker response, following more than 200 ms after stimulation (see example in Fig. 5). This delayed response component may reflect a stimulus-evoked UP state (Anderson et al. 2000; Hasenstaub et al. 2007; Reig and Sanchez-Vives 2007; Alenda et al. 2010), which often originates in more frontal cortical regions (Massimini et al. 2004; Ruiz-Mejias et al. 2011). Another possibility might be the delayed protraction of the whiskers following the initial air puff. Such forward movement of the whiskers is controlled by M1 (Matyas et al. 2010) and might underlie the delayed activation of M1 under our experimental conditions as well. Our data showed that M1 did not contribute to dorsolateral striatal tactile responses, but it may play an important role in active whisking (Szwed et al. 2003) in awake mice.

Cortical and Thalamic Striatal Afferents

In addition to corticostriatal projections, striatal neurons receive excitatory input from the thalamus (Cheatwood et al. 2005; Alloway et al. 2006; Lacey et al. 2007; Doig et al. 2010; Smith et al. 2012; Parker et al. 2016). In our experiments, we did not observe a direct thalamic input that could act as a shortcut, arriving earlier to MSNs in dorsal striatum. Inactivation of the neocortical S1 caused large reductions in striatal response. In particular, responses to contralateral whisker deflection were reduced by more than 80% after inactivation of ipsilateral S1 (Fig. 6). Moreover, onset latencies of whisker responses were longer than those in cortical neurons (Fig. 1, and see also Reig and Silberberg 2014). Those results support the dominance of cortical excitation in mediating the whisker-evoked responses under our experimental conditions. Repetitive whisker stimulation evoked extracellular responses in rat dorsolateral striatum with earlier discharge onsets than those observed in S1 (Mowery et al. 2011; Smith et al. 2012). These early responses were suggested to be mediated by whisker-evoked thalamostriatal input from posteromedial complex (POM) (Mowery et al. 2011; Smith et al. 2012). Reasons for these differences may lie in the respective experimental settings such as anesthetics,

species, and stimulus type, as previously discussed (Smith et al. 2012). Whisker deflection was previously shown to evoke only weak responses in POM neurons under ketamine and urethane anesthesia (Diamond et al. 1992; Lavallee et al. 2005). It is possible that similar experiments under light isoflurane anesthesia (Mowery et al. 2011) would result in different activation of POM. Moreover, input from thalamic nuclei is heterogeneous, with responses mediated via NMDA receptors (Ellender et al. 2013), which are reduced by ketamine anesthesia. In our study, whisker pads were activated monophasically by a single air puff, as opposed to experiments using repetitive bidirectional whisker deflections, which activate different pathways from S1 and motor cortices upon retraction or protraction (Matyas et al. 2010) and may underlie the observed short response latencies (Smith et al. 2012). Another intriguing mechanism that may support the cortical dominance following transient sensory input is heterosynaptic suppression of thalamic input (Calhoon and O'Donnell 2013). TTX in S1 blocked most of the contralateral whisker responses and we did not identify an early thalamic component that acted as a "shortcut" preceding the cortical input, however, the properties of thalamostriatal inputs remain to be elucidated in the awake animal, aided by molecular differentiation of the respective excitatory inputs. Striatal neurons were shown to receive inputs from various presynaptic structures in the cortex, thalamus, as well as other subcortical structures in the brainstem and within the basal ganglia (Mallet et al. 2012; Wall et al. 2013; Dautan et al. 2014; Glajch et al. 2016). These pathways to striatal neurons may play a role in mediating the compound delayed responses to whisker stimulation via parallel polysynaptic pathways but are beyond the scope of this study. In this study, we focused on the earlier components of striatal responses, which were mostly mediated by cortical inputs. In order to understand delayed response components as well as the ongoing activity of striatal neurons under physiological conditions, it is important to also dissect the various subcortical afferent pathways.

Sensory Responses in Different Striatal Neuron Types

In this study, we recorded from MSNs without separating them into direct (dMSN) and indirect (iMSN) subpopulations. We have recently shown that MSNs of both types respond to bilateral whisker stimulation, however, there were differences between dMSNs and iMSNs in their respective responses to ipsi- and contralateral whisker stimuli (Reig and Silberberg 2014). In particular, dMSNs had larger amplitude and latency differences between contra- and ipsilateral responses, which may be caused by differences in afferent pathways. Recent studies support these findings by showing that dMSNs receive stronger input from ipsilateral cortex (Kress et al. 2013), and from a larger proportion of presynaptic cells in ipsilateral S1 (Wall et al. 2013). We showed earlier that whisker responses were observed in fast-spiking and cholinergic interneurons (Reig and Silberberg 2014), however, due to their small fraction within the striatal network, we did not perform any TTX inactivation experiments while recording from interneurons. Previous work showed that different interneuron types receive diverse forms of cortical and thalamic excitatory inputs (Lapper and Bolam 1992; Ding et al. 2010; Sharott et al. 2012; Doig et al. 2014). It still remains to be seen how sensory integration differs for the various interneuron types as well as between striatal matrix and striosomal compartments (Malach and Graybiel

1986; Friedman et al. 2015). In order to fully understand the function of the various corticostriatal pathways, it will be crucial to unravel the anatomical and synaptic properties of striatal afferents to the different neuronal subtypes in the striatum.

Supplementary Material

Supplementary material can be found at: http://www.cercor. oxfordjournals.org/

Funding

Notes

References

Akers RM, Killackey HP. 1978. Organization of corticocortical connections in the parietal cortex of the rat. J Comp Neurol. 181:513–537.

Alenda A, Molano-Mazon M, Panzeri S, Maravall M. 2010. Sensory input drives multiple intracellular information streams in somatosensory cortex. J Neurosci. 30:10872–10884.

Alloway KD. 2008. Information processing streams in rodent barrel cortex: the differential functions of barrel and septal circuits. Cereb Cortex. 18:979–989.

Alloway KD, Crist J, Mutic JJ, Roy SA. 1999. Corticostriatal projections from rat barrel cortex have an anisotropic organization that correlates with vibrissal whisking behavior. J Neurosci. 19:10908–10922.

Alloway KD, Lou L, Nwabueze-Ogbo F, Chakrabarti S. 2006. Topography of cortical projections to the dorsolateral neostriatum in rats: multiple overlapping sensorimotor pathways. J Comp Neurol. 499:33–48.

Alloway KD, Smith JB, Beauchemin KJ, Olson ML. 2009. Bilateral projections from rat MI whisker cortex to the neostriatum, thalamus, and claustrum: forebrain circuits for modulating whisking behavior. J Comp Neurol. 515:548–564.

Alloway KD, Smith JB, Watson GD. 2014. Thalamostriatal projections from the medial posterior and parafascicular nuclei have distinct topographic and physiologic properties. J Neurophysiol. 111:36–50.

Anderson J, Lampl I, Reichova I, Carandini M, Ferster D. 2000. Stimulus dependence of two-state fluctuations of membrane potential in cat visual cortex. Nat Neurosci. 3:617–621.

Brown LL, Hand PJ, Divac I. 1996. Representation of a single vibrissa in the rat neostriatum: peaks of energy metabolism reveal a distributed functional module. Neuroscience. 75: 717–728.

Calhoon GG, O'Donnell P. 2013. Closing the gate in the limbic striatum: prefrontal suppression of hippocampal and thalamic inputs. Neuron. 78:181–190.

Carman JB, Cowan WM, Powell TP, Webster KE. 1965. A bilateral cortico-striate projection. J Neurol Neurosurg Psychiatry. 28:71–77.

Cheatwood JL, Corwin JV, Reep RL. 2005. Overlap and interdigitation of cortical and thalamic afferents to dorsocentral striatum in the rat. Brain Res. 1036:90–100.

Cui G, Jun SB, Jin X, Pham MD, Vogel SS, Lovinger DM, Costa RM. 2013. Concurrent activation of striatal direct and indirect pathways during action initiation. Nature. 494:238–242.

Dautan D, Huerta-Ocampo I, Witten IB, Deisseroth K, Bolam JP, Gerdjikov T, Mena-Segovia J. 2014. A major external source of cholinergic innervation of the striatum and nucleus accumbens originates in the brainstem. J Neurosci. 34:4509–4518.

de Kock CP, Bruno RM, Spors H, Sakmann B. 2007. Layer- and cell-type-specific suprathreshold stimulus representation in rat primary somatosensory cortex. J Physiol. 581:139–154.

Diamond ME, Armstrong-James M, Ebner FF. 1992. Somatic sensory responses in the rostral sector of the posterior group (POm) and in the ventral posterior medial nucleus (VPM) of the rat thalamus. J Comp Neurol. 318:462–476.

Ding JB, Guzman JN, Peterson JD, Goldberg JA, Surmeier DJ. 2010. Thalamic gating of corticostriatal signaling by cholinergic interneurons. Neuron. 67:294–307.

Doig NM, Magill PJ, Apicella P, Bolam JP, Sharott A. 2014. Cortical and thalamic excitation mediate the multiphasic responses of striatal cholinergic interneurons to motivationally salient stimuli. J Neurosci. 34:3101–3117.

Doig NM, Moss J, Bolam JP. 2010. Cortical and thalamic innervation of direct and indirect pathway medium-sized spiny neurons in mouse striatum. J Neurosci. 30:14610–14618.

Donoghue JP, Herkenham M. 1986. Neostriatal projections from individual cortical fields conform to histochemically distinct striatal compartments in the rat. Brain Res. 365:397–403.

Ellender TJ, Harwood J, Kosillo P, Capogna M, Bolam JP. 2013. Heterogeneous properties of central lateral and parafascicular thalamic synapses in the striatum. J Physiol. 591:257–272.

Ferezou I, Bolea S, Petersen CC. 2006. Visualizing the cortical representation of whisker touch: voltage-sensitive dye imaging in freely moving mice. Neuron. 50:617–629.

Friedman A, Homma D, Gibb LG, Amemori K, Rubin SJ, Hood AS, Riad MH, Graybiel AM. 2015. A corticostriatal path targeting striosomes controls decision-making under conflict. Cell. 161:1320–1333.

Glajch KE, Kelver DA, Hegeman DJ, Cui Q, Xenias HS, Augustine EC, Hernandez VM, Verma N, Huang TY, Luo M, et al. 2016. Npas1+ pallidal neurons target striatal projection neurons. J Neurosci. 36:5472–5488.

Graybiel AM, Ragsdale CWJr. 1979. Fiber connections of the basal ganglia. Prog Brain Res. 51:237–283.

Hasenstaub A, Sachdev RN, McCormick DA. 2007. State changes rapidly modulate cortical neuronal responsiveness. J Neurosci. 27:9607–9622.

Hoffer ZS, Arantes HB, Roth RL, Alloway KD. 2005. Functional circuits mediating sensorimotor integration: quantitative comparisons of projections from rodent barrel cortex to primary motor cortex, neostriatum, superior colliculus, and the pons. J Comp Neurol. 488:82–100.

Hoover JE, Hoffer ZS, Alloway KD. 2003. Projections from primary somatosensory cortex to the neostriatum: the role of somatotopic continuity in corticostriatal convergence. J Neurophysiol. 89:1576–1587.

Hubener M, Bolz J. 1988. Morphology of identified projection neurons in layer 5 of rat visual cortex. Neurosci Lett. 94:76–81.

Innocenti GM, Manger PR, Masiello I, Colin I, Tettoni L. 2002. Architecture and callosal connections of visual areas 17, 18, 19 and 21 in the ferret (Mustela putorius). Cereb Cortex. 12:411–422.

Khibnik LA, Tritsch NX, Sabatini BL. 2014. A direct projection from mouse primary visual cortex to dorsomedial striatum. PLoS One. 9:e104501.

Kincaid AE, Wilson CJ. 1996. Corticostriatal innervation of the patch and matrix in the rat neostriatum. J Comp Neurol. 374:578–592.

Kress GJ, Yamawaki N, Wokosin DL, Wickersham IR, Shepherd GM, Surmeier DJ. 2013. Convergent cortical innervation of striatal projection neurons. Nat Neurosci. 16:665–667.

Kunzle H. 1975. Bilateral projections from precentral motor cortex to the putamen and other parts of the basal ganglia. An autoradiographic study in Macaca fascicularis. Brain Res. 88:195–209.

Lacey CJ, Bolam JP, Magill PJ. 2007. Novel and distinct operational principles of intralaminar thalamic neurons and their striatal projections. J Neurosci. 27:4374–4384.

Lapper SR, Bolam JP. 1992. Input from the frontal cortex and the parafascicular nucleus to cholinergic interneurons in the dorsal striatum of the rat. Neuroscience. 51:533–545.

Lavallee P, Urbain N, Dufresne C, Bokor H, Acsady L, Deschenes M. 2005. Feedforward inhibitory control of sensory information in higher-order thalamic nuclei. J Neurosci. 25:7489–7498.

Le Be JV, Silberberg G, Wang Y, Markram H. 2007. Morphological, electrophysiological, and synaptic properties of corticocallosal pyramidal cells in the neonatal rat neocortex. Cereb Cortex. 17:2204–2213.

Malach R, Graybiel AM. 1986. Mosaic architecture of the somatic sensory-recipient sector of the cat's striatum. J Neurosci. 6:3436–3458.

Mallet N, Micklem BR, Henny P, Brown MT, Williams C, Bolam JP, Nakamura KC, Magill PJ. 2012. Dichotomous organization of the external globus pallidus. Neuron. 74:1075–1086.

Massimini M, Huber R, Ferrarelli F, Hill S, Tononi G. 2004. The sleep slow oscillation as a traveling wave. J Neurosci. 24:6862–6870.

Matyas F, Sreenivasan V, Marbach F, Wacongne C, Barsy B, Mateo C, Aronoff R, Petersen CC. 2010. Motor control by sensory cortex. Science. 330:1240–1243.

McGeorge AJ, Faull RL. 1987. The organization and collateralization of corticostriate neurones in the motor and sensory cortex of the rat brain. Brain Res. 423:318–324.

McGeorge AJ, Faull RL. 1989. The organization of the projection from the cerebral cortex to the striatum in the rat. Neuroscience. 29:503–537.

Morishima M, Kawaguchi Y. 2006. Recurrent connection patterns of corticostriatal pyramidal cells in frontal cortex. J Neurosci. 26:4394–4405.

Mowery TM, Harrold JB, Alloway KD. 2011. Repeated whisker stimulation evokes invariant neuronal responses in the dorsolateral striatum of anesthetized rats: a potential correlate of sensorimotor habits. J Neurophysiol. 105:2225–2238.

Parker PR, Lalive AL, Kreitzer AC. 2016. Pathway-specific remodeling of thalamostriatal synapses in parkinsonian mice. Neuron. 89:734-740.

Pidoux M, Mahon S, Deniau JM, Charpier S. 2011. Integration and propagation of somatosensory responses in the corticostriatal pathway: an intracellular study in vivo. J Physiol. 589:263–281.

Reig R, Sanchez-Vives MV. 2007. Synaptic transmission and plasticity in an active cortical network. PLoS One. 2:e670.

Reig R, Silberberg G. 2014. Multisensory integration in the mouse striatum. Neuron. 83:1200–1212.

Ruiz-Mejias M, Ciria-Suarez L, Mattia M, Sanchez-Vives MV. 2011. Slow and fast rhythms generated in the cerebral cortex of the anesthetized mouse. J Neurophysiol. 106: 2910–2921.

Seamari Y, Narvaez JA, Vico FJ, Lobo D, Sanchez-Vives MV. 2007. Robust off- and online separation of intracellularly recorded up and down cortical states. PLoS One. 2:e888.

Sharott A, Doig NM, Mallet N, Magill PJ. 2012. Relationships between the firing of identified striatal interneurons and spontaneous and driven cortical activities in vivo. J Neurosci. 32:13221–13236.

Shepherd GM. 2013. Corticostriatal connectivity and its role in disease. Nat Rev Neurosci. 14:278–291.

Shuler MG, Krupa DJ, Nicolelis MA. 2001. Bilateral integration of whisker information in the primary somatosensory cortex of rats. J Neurosci. 21:5251–5261.

Sippy T, Lapray D, Crochet S, Petersen CC. 2015. Cell-type-specific sensorimotor processing in striatal projection neurons during goal-directed behavior. Neuron. 88:298–305.

Smith AD, Bolam JP. 1990. The neural network of the basal ganglia as revealed by the study of synaptic connections of identified neurones. Trends Neurosci. 13:259–265.

Smith JB, Mowery TM, Alloway KD. 2012. Thalamic POm projections to the dorsolateral striatum of rats: potential pathway for mediating stimulus-response associations for sensorimotor habits. J Neurophysiol. 108:160–174.

Szwed M, Bagdasarian K, Ahissar E. 2003. Encoding of vibrissal active touch. Neuron. 40:621–630.

Wall NR, De La Parra M, Callaway EM, Kreitzer AC. 2013. Differential innervation of direct- and indirect-pathway striatal projection neurons. Neuron. 79:347–360.

Welker E, Hoogland PV, Van der Loos H. 1988. Organization of feedback and feedforward projections of the barrel cortex: a PHA-L study in the mouse. Exp Brain Res. 73:411–435.

Wilson CJ. 1987. Morphology and synaptic connections of crossed corticostriatal neurons in the rat. J Comp Neurol. 263:567–580.

Wise SP, Jones EG. 1976. The organization and postnatal development of the commissural projection of the rat somatic sensory cortex. J Comp Neurol. 168:313–343.

Wright AK, Ramanathan S, Arbuthnott GW. 2001. Identification of the source of the bilateral projection system from cortex to somatosensory neostriatum and an exploration of its physiological actions. Neuroscience. 103:87–96.

Znamenskiy P, Zador AM. 2013. Corticostriatal neurons in auditory cortex drive decisions during auditory discrimination. Nature. 497:482–485.